

## NMR Conformational Study Reveals that S-C-N Anomeric Effect in Thionucleosides Is Weaker than O-C-N Anomeric Effect in Natural Nucleosides

Martin Črnugelj and Janez Plavec\*

NMR Center, National Institute of Chemistry, Hajdrihova 19,  
SI-1115 Ljubljana, Slovenia

Received November 13, 2000; revised January 11, 2001; accepted January 16, 2001

The comparative analysis by NMR and *ab initio* calculations of the energetics of North  $\rightleftharpoons$  South pseudorotational equilibrium in 4'-thionucleosides and in their natural 4'-oxo counterparts has shown that S-C-N anomeric effect in the former is weaker than O-C-N anomeric effect in the latter. The  $\Delta\Delta H^\circ$  values between 2'-deoxy-4'-thio analogues and their 4'-oxo counterparts after accounting for the drive by 3'-OH group have been attributed to the weakening of the nucleobase-dependent S4'-C1'-N9/1 anomeric effect by 3.3, 6.5, 8.5 and 9.2 kJ mol<sup>-1</sup> in adenine, guanine, cytosine and thymine, respectively. In addition, S-C-N anomeric effect is stronger in purine than in pyrimidine 4'-thionucleosides and increases in the following order: thymine < cytosine < guanine < adenine, which is in contrast to natural nucleosides.

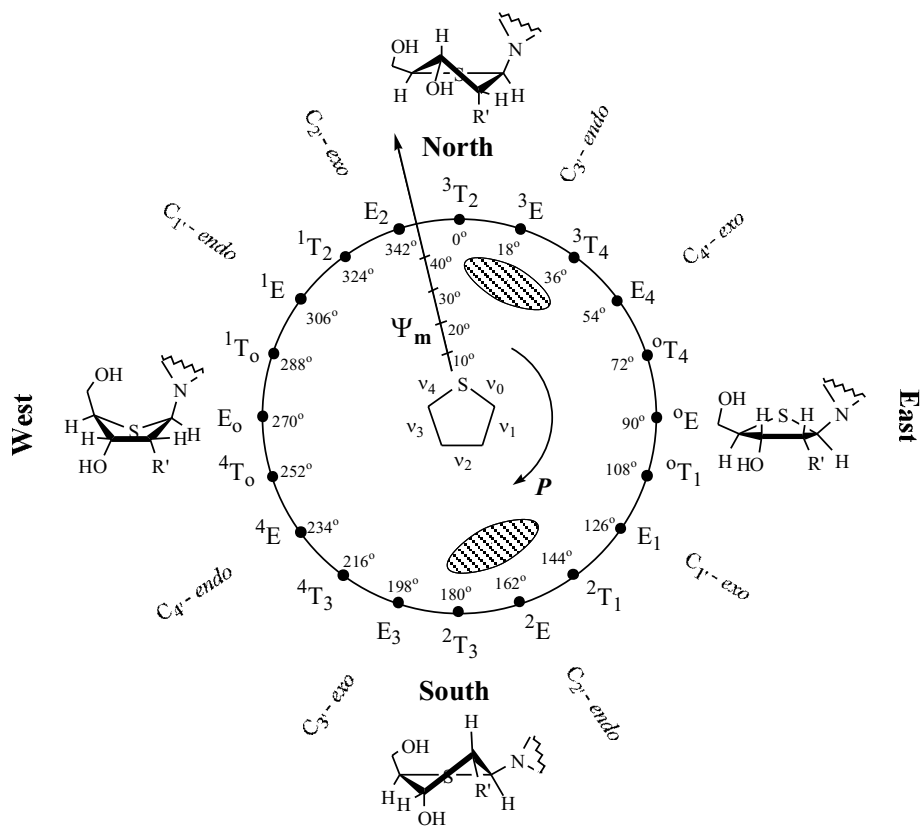
*Key words:* NMR, nucleoside, conformational analysis, anomeric effect, pseudorotational equilibrium.

### INTRODUCTION

The pentofuranosyl moieties of natural nucleosides and nucleotides adopt a variety of distinct puckered conformations (Scheme 1).<sup>1</sup> Extensive studies by X-ray crystallography, NMR spectroscopy and computational methods have established that the sugar moieties of nucleos(t)ides are in solution involved in a two-state conformational equilibrium (shaded areas in Scheme

\* Author to whom correspondence should be addressed. (E-mail: janez.plavec@ki.si)

1). Two distinctly identifiable conformations are denoted as North (N) and South (S).<sup>2,3</sup> The two-state  $N \rightleftharpoons S$  pseudorotational equilibrium is controlled by the competing anomeric and *gauche* effects.<sup>4-24</sup> The 2'-OH and 3'-OH groups drive  $N \rightleftharpoons S$  equilibrium through the tendency to adopt a *gauche* arrangement of [O4'-C1'-C2'-O2'], [N9/1-C1'-C2'-O2'] and [O4'-C4'-C3'-O3'] fragments.<sup>4</sup> The heterocyclic nucleobase drives  $N \rightleftharpoons S$  equilibrium by two counteracting contributions from (i) the inherent steric effect of the nucleobase,<sup>10,13,25</sup> and (ii) the anomeric effect.



Scheme 1

The anomeric effect describes the empirical observation of a preference for electronegative exocyclic substituents to occupy the pseudoaxial over the pseudoequatorial position at the anomeric carbon,<sup>26-29</sup> and results in the preference for N-type (pseudoaxial aglycon) over S-type (pseudoequatorial aglycon) conformation. The origin of the O-C-N anomeric effect can be described by (i) the higher dipole-dipole electrostatic repulsions which destabi-

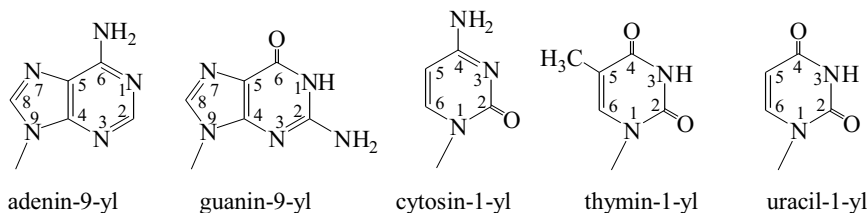
lise the pseudoequatorial orientation (S-type sugar) of aglycon at C1', and (ii) a favourable overlap between electron pair orbital of the endocyclic O4' and the vacant antibonding  $\sigma^*$  orbital of the glycosidic bond which results in the stabilisation of the pseudoaxially oriented nucleobase (N-type sugar). Whatever the origin is, the O4'-C1'-N anomeric effect in nucleosides varies with the diversity of  $\pi$ -electron systems of purine and pyrimidine nucleobases, which can be in addition modulated by substitution, and is uniformly strengthened by the protonation of the nucleobase.<sup>16,17</sup> Similarly, the replacement of endocyclic oxygen with methylene group<sup>24,25</sup> or sulphur<sup>8,30</sup> atom causes a significant electronic and structural changes that alter the drive of  $N \rightleftharpoons S$  equilibrium by the heterocyclic aglycon and thus enable new insights into the O-C-N anomeric effect in natural nucleosides.

We have described a detailed temperature- and pH-dependent <sup>1</sup>H NMR conformational study of a series of 4'-thio- $\beta$ -D-2'-deoxyribonucleosides **1–4** and their ribo counterparts **5–8** in D<sub>2</sub>O in our previous work.<sup>30</sup> Here we have compared the energetics of their  $N \rightleftharpoons S$  equilibria to assess the effect of bond distance changes as well as electronic changes caused by replacement of oxygen with sulphur atom on the strength of the anomeric effect in nucleosides in order to get a semiquantitative measure of S4'-C1'-N *vs.* O4'-C1'-N anomeric effect in both 2'-deoxy- and ribo analogues (Scheme 2).

It is important to rationalise and quantitate the steric and electronic forces that are introduced by substitution of oxygen by sulphur and might



- |   |   |
|---|---|
| <b>1:</b> tA (X = S), dA (X = O) (Base = adenin-9-yl)   | <b>5:</b> tA (X = S), A (X = O) (Base = adenin-9-yl)  |
| <b>2:</b> tdG (X = S), dG (X = O) (Base = guanin-9-yl)  | <b>6:</b> tG (X = S), G (X = O) (Base = guanin-9-yl)  |
| <b>3:</b> tdC (X = S), dC (X = O) (Base = cytosin-1-yl) | <b>7:</b> tC (X = S), C (X = O) (Base = cytosin-1-yl) |
| <b>4:</b> tdT (X = S), T (X = O) (Base = thymine-1-yl)  | <b>8:</b> tU (X = S), U (X = O) (Base = uracil-1-yl)  |



Scheme 2

have important biological and chemical consequences in many classes of compounds, *e.g.* in thiocarbohydrates,<sup>31</sup> in 4'-thionucleosides alone<sup>32</sup> or when incorporated in antisense oligonucleosides.<sup>33</sup> The knowledge and rationalisation of conformational changes due to replacement of ring oxygen with homologous second row element should help to understand the properties and functions of the ring oxygen atom.

## EXPERIMENTAL

### *NMR Spectroscopy*

<sup>1</sup>H-NMR spectra were recorded at 299.94 MHz on Varian Unity Plus and at 600.11 MHz on Varian Unity Inova NMR spectrometers at the National NMR Center of Slovenia. Spectra were acquired in D<sub>2</sub>O (99.9% deuterium) at neutral pH (6.5–7.8) at five temperatures from 278 K to 358 K in 20 K steps. The sample temperature was controlled to approximately ±0.5 K. Sample concentration was 1 × 10<sup>-2</sup> mol dm<sup>-3</sup> for tdC (**3**), tdT (**4**), tC (**7**) and tU (**8**), 5 × 10<sup>-3</sup> mol dm<sup>-3</sup> for tdG (**2**) and tG (**6**), 2.5 × 10<sup>-3</sup> mol dm<sup>-3</sup> for tdA (**1**) and tA (**5**) due to poor solubility. The measurements were performed under the following spectral and processing conditions: 3500 Hz sweep width, 16 K time domain, zero filling to 64 K, and slight gaussian apodization to give enhanced resolution. The basic assignment of the strongly coupled and partly overlapped resonances was performed with the use of selective decoupling. In order to obtain accurate *J*-coupling data and chemical shifts <sup>1</sup>H NMR spectra were simulated with a standard computer simulation algorithm, which is integrated into Varian software (VNMR rev. 6.1A).<sup>34</sup> The error in <sup>3</sup>J<sub>HH</sub> is smaller than 0.1 Hz as estimated from the comparison of the experimental and simulated spectra.

### *Conformational Analysis of <sup>3</sup>J<sub>HH</sub> Proton-Proton Coupling Constants*

The conformational analysis of the 4'-thiofuranose moiety in **1–8** has been performed with the use of computer program PSEUROT,<sup>35</sup> which finds the best fit between experimental and calculated <sup>3</sup>J<sub>HH</sub> coupling constants, and consists of three essential translation steps. The first step translates coupling constants of vicinal protons to proton-proton torsion angles and is covered by the generalised Karplus-Altorna equation.<sup>36,37</sup> We have taken particular care to account for the substitution of O4' in the natural pentofuranosyl moiety with a sulphur atom in **1–8**. The second step is the translation of proton-proton torsion angles into the corresponding endocyclic torsion angles and is formulated with the set of linear equations  $\Phi_{\text{HH}} = Av_j + B$ .  $\Phi_{\text{HH}}$  is the torsion angle between two vicinal protons and  $v_j$  is the corresponding endocyclic torsion angle.<sup>38</sup> Parameters *A* and *B* are corrections for non-ideality of Newman projection symmetry and have been determined for **1–8** with the use of *ab initio* optimised geometries at HF/3-21G level. The third translational step of endocyclic torsion angles into the pseudorotational parameters is described by a simple cosine function (1).

$$v_j = a_j * \Psi_m * \cos[P + \varepsilon_j + 4\pi/5 * (j-2)] \cdots 0 \leq j \leq 4 \quad (1)$$

$P$  is the phase angle of pseudorotation and  $\Psi_m$  is the maximum puckering amplitude. The parameters  $a_j$  and  $\varepsilon_j$  have been introduced<sup>39</sup> due to unequilateral 4'-thiofuranose ring, and were in this work calculated from *ab initio* optimised geometries of 31 conformers of tdG (**2**) and  $\beta$ -tdU, and 28 conformers of tG (**6**) and tU (**8**). The input for PSEUROT program consists of the parameters  $P_1$ - $P_6$  for the generalised Karplus-Altona equation, the  $\lambda$  electronegativities of the four substituents,  $A$ ,  $B$ ,  $a_j$  and  $\varepsilon_j$  parameters (Table I), temperature-dependent experimental  ${}^3J_{\text{HH}}$  and the initial guesses of the geometries of the starting conformers and their respective populations. The following  $\lambda$  electronegativity values were used: 0.0 for H, 1.26 for OH, 0.62 for C1', C2', C3' and C4', 0.68 for C5', 0.70 for S and 0.58 for the nucleobase.<sup>37</sup> The discrepancy between the experimental and calculated  ${}^3J_{\text{HH}}$  has been monitored through the calculation of root-mean-square error. Despite a slight bias of N  $\rightleftharpoons$  S pseudorotational equilibrium towards S-type conformers in **1-4**, we have constrained  $\Psi_m^{\text{N}}$  and  $\Psi_m^{\text{S}}$  during the iteration procedure. The same procedure was used for **5-8**, where population of N- and S- type pseudorotamers was approximately equal. In order to find the global minimum, we have systematically varied  $\Psi_m^{\text{N}}$  and  $\Psi_m^{\text{S}}$  from 39° to 50° in 1° steps.

TABLE I

Parameters  $A$ ,  $B$ ,  $a_j$  and  $\varepsilon_j$  calculated from the *ab initio* (3-21G, 6-31G\*\*) optimised geometries<sup>a</sup>

proton pair	2'-deoxy-4'-thio <sup>b</sup>				4'-thio <sup>c</sup>			
	$A$	$B$	$a_j$	$\varepsilon_j$	$A$	$B$	$a_j$	$\varepsilon_j$
H1'-H2'	1.049	120.58°	0.9475	0.6°	1.058	121.88°	1.0318	4.1°
H1'-H2''	1.026	0.95°	1.0314	4.1°				
H2'-H3'	1.087	1.65°	1.0386	0.0°	1.108	-1.19°	1.0371	0.0°
H2''-H3'	1.063	120.71°	1.0361	-4.3°				
H3'-H4'	1.017	-123.67°	0.9544	-0.8°	1.023	-123.51°	1.0349	-4.0°

<sup>a</sup> Parameters  $A$  and  $B$  have been derived from the set of  $\Phi_{\text{HH}}$  and  $\nu_j$  torsions angles using the equation:  $\Phi_{\text{HH}} = A\nu_j + B$ . All relations showed the Pearson correlation coefficient higher than 0.997.

<sup>b</sup>  $A$ ,  $B$ ,  $a_j$  and  $\varepsilon_j$  for 2'-deoxy-4'-thioribofuranosyl ring have been calculated from 31 conformers of tdG(**2**) and  $\beta$ -tdU.

<sup>c</sup>  $A$ ,  $B$ ,  $a_j$  and  $\varepsilon_j$  for 4'-thioribofuranosyl ring have been calculated from 28 conformers of tG(**6**) and tU (**8**).

### Ab initio MO Calculations

All calculations were performed with GAUSSIAN 94 (Ref. 40) and 98 (Ref. 41) programs running on a Silicon Graphics Indigo 2 with an R4000 processor and IRIS Origin 2000 with four R10000 processors. For all the pseudorotamers all internal degrees of freedom were first freely optimised at Hartree-Fock (HF) level of theory us-

ing the standard 3-21G basis set. HF/3-21G optimised geometries of the N-, E- and S-type conformers were used as input for geometry optimisations at HF/6-31G\*\* level (from 319 to 369 basis functions). Stationary points were verified through vibrational frequency calculations.

## RESULTS

### *North* $\rightleftharpoons$ *South* Pseudorotational Equilibrium in **1–8**

The analysis of solution conformation of 4'-thioribofuranosyl ring in **1–8** is based on  ${}^3J_{1'2'}$ ,  ${}^3J_{1'2''}$ ,  ${}^3J_{2'3'}$ ,  ${}^3J_{2'3''}$  and  ${}^3J_{3'4'}$  proton-proton coupling constants acquired at five temperatures in the range from 278 K to 358 K in 20 K steps. The precise values for coupling constants and chemical shifts were obtained through the simulation and iteration procedure.<sup>34</sup> The chemical shifts at 298 K and  ${}^3J_{\text{HH}}$  vicinal coupling constants at two limiting temperatures are given in Tables II and III, respectively.

TABLE II  
 ${}^1\text{H}$  NMR chemical shifts at 298 K at neutral pH for **1–8**<sup>a</sup>

Compd.	H8	H2	H6	H5	CH <sub>3</sub>	H1'	H2'	H2''	H3'	H4'	H5'	H5''
tdA ( <b>1</b> )	8.51	8.25				6.72	2.71	2.71	HOD <sup>a</sup>	3.62	3.94	3.86
tdG ( <b>2</b> )	8.14					6.11	2.64	2.66	4.63	3.58	3.92	3.84
tdC ( <b>3</b> )			8.10	6.08		6.29	2.30	2.51	4.52	3.51	3.84	3.77
tdT ( <b>4</b> )			7.91		1.92	6.32	2.32	2.48	4.56	3.52	3.85	3.80
tA ( <b>5</b> )	8.54	8.27				5.97	HOD <sup>a</sup>		4.37	3.62	4.01	3.93
tG ( <b>6</b> )	8.18					5.79	4.67		4.36	3.58	3.98	3.90
tC ( <b>7</b> )			8.19	6.09		5.98	4.36		4.19	3.51	3.93	3.84
tU ( <b>8</b> )			8.21	5.93		5.98	4.39		4.22	3.50	3.91	3.84

<sup>a</sup> H2/H3' are hidden under water signal ( $\delta \approx 4.79$  ppm).

The temperature-dependent  ${}^3J_{\text{HH}}$  coupling constants have been analysed with the use of the computer program PSEUROT<sup>42</sup> which calculates the least-squares fit of the five parameters defining the two state N  $\rightleftharpoons$  S equilibrium ( $P_{\text{N}}$ ,  $\Psi_{\text{m}}^{\text{N}}$ ,  $P_{\text{S}}$ ,  $\Psi_{\text{m}}^{\text{S}}$  and  $x_{\text{S}}$ ) to the set of experimental  ${}^3J_{\text{HH}}$ . The conformational analyses of **1–4** have been performed by constraining  $\Psi_{\text{m}}^{\text{N}}$  and  $\Psi_{\text{m}}^{\text{S}}$  to fixed values between 39° and 50° while optimising the phase angles of pseudorotation and respective populations of N- and S-type pseudo-

TABLE III

Experimental  ${}^3J_{\text{HH}}$  proton-proton coupling constants and conformational equilibrium across C4'-C5' bond in **1–8** at two limiting temperatures in D<sub>2</sub>O<sup>a</sup>

Compd.	T/K	${}^3J_{1'2'}$	${}^3J_{1'2''}$	${}^3J_{2'3''}$	${}^3J_{2'3'}$	${}^3J_{3'4'}$	${}^3J_{4'5'}$	${}^3J_{4'5''}$	% $\gamma^+$	% $\gamma^-$	% $\gamma^t$
tdA ( <b>1</b> ) <sup>b</sup>	278	12.6		14.4	4.3	5.7	5.8		34	32	33
	358	13.1		14.3	4.1	6.0	6.0		30	35	35
tdG ( <b>2</b> )	278	6.9	6.7	5.1	4.4	4.0	6.1	6.1	28	36	36
	338	6.7	6.8	5.3	4.4	4.0	6.1	6.2	27	36	37
tdC ( <b>3</b> )	278	7.3	6.8	4.3	4.9	3.7	6.4	6.1	26	39	35
	358	7.0	6.9	4.6	5.2	4.0	6.2	6.2	26	37	37
tdT ( <b>4</b> )	278	8.0	6.7	4.3	4.2	3.1	6.4	5.8	28	40	32
	358	7.5	6.9	4.5	4.7	3.6	6.2	6.0	28	37	35
tA ( <b>5</b> )	278	5.0		3.6		5.2	4.8	5.4	46	23	31
	358	5.5		3.8		4.6	5.3	5.9	37	28	35
tG ( <b>6</b> )	278	5.5		3.6		4.9	5.2	5.7	40	27	33
	358	5.7		3.8		4.5	5.5	6.0	34	30	36
tC ( <b>7</b> )	278	5.0		3.6		5.5	4.9	5.5	44	24	32
	358	5.5		3.9		5.0	5.4	5.9	36	29	35
tU ( <b>8</b> )	278	5.6		3.7		4.8	5.2	5.4	42	28	30
	358	6.0		3.8		4.3	5.5	5.8	36	30	34

<sup>a</sup>  ${}^3J_{\text{HH}}$  values (in Hz,  $\pm 0.1$  Hz) have been extracted from 1D <sup>1</sup>H NMR spectra recorded at 300 MHz in D<sub>2</sub>O between 278 and 358 K in 20 K steps, except for tdG (**2**), where spectra were recorded at 600 MHz between 278 and 338 K in 20 K steps. The complete set of  $J_{\text{HH}}$  coupling constants and chemical shifts at all temperatures has been simulated.

<sup>b</sup> Resonances of H2' and H2'' in tdA (**1**) were isochronous and only the sums of proton-proton coupling constants ( $\Sigma 1'$  and  $\Sigma 3'$ ) could be extracted and used in the conformational analysis.

rotamers. After convergence we obtained the best fits between experimental and back-calculated  ${}^3J_{\text{HH}}$  (root-mean-square error < 0.18 Hz,  $\Delta J^{\text{max}} < 0.3$  Hz) for the N  $\rightleftharpoons$  S pseudorotational equilibria in **1–4**. The results in Table IV show that the geometries of N-type conformers in **1–4** were characterised by the puckering between C3'-*endo*, C2'-*exo* twist and C3'-*endo* envelope canonical forms ( $0^\circ < P_{\text{N}} < 20^\circ$ ), whereas their partners in the S region of conformational space exhibited puckering between C2'-*endo* envelope and C2'-*endo*, C3'-*exo* twist canonical forms ( $151^\circ < P_{\text{S}} < 185^\circ$ ).

The conformational analyses of  ${}^3J_{\text{HH}}$  coupling constants in 4'-thioribofuranosyl nucleosides **5–8** have shown approximately equal populations of N- and S-type pseudorotamers at 298 K at the best fits between experimental

TABLE IV

The population of South-type conformers, geometries and thermodynamic parameters for the N  $\rightleftharpoons$  S pseudorotational equilibrium in **1–8**<sup>a</sup>

Compd.	%S(298 K)	$P_N$	$\Psi_m^N$	$P_S$	$\Psi_m^S$	$\Delta H^\circ$	$\Delta S^\circ$	$\Delta G^\circ$
tdA ( <b>1</b> )	57	-1	46 <sup>b</sup>	185	46 <sup>b</sup>	0.8 (0.1)	4.9 (0.6)	-0.7 (0.1)
tdG ( <b>2</b> )	62	11	39 <sup>b</sup>	151	39 <sup>b</sup>	-0.7 (0.1)	1.7 (0.1)	-1.2 (0.1)
tdC ( <b>3</b> )	63	16	43 <sup>b</sup>	170	43 <sup>b</sup>	-1.4 (0.1)	-0.3 (0.1)	-1.3 (0.1)
tdT ( <b>4</b> )	70	20	43 <sup>b</sup>	170	43 <sup>b</sup>	-2.7 (0.1)	-2.2 (0.1)	-2.0 (0.1)
tA ( <b>5</b> )	54	10	44 <sup>b</sup>	158	44 <sup>b</sup>	2.9 (0.2)	11.1 (2.3)	-0.6 (0.6)
tG ( <b>6</b> )	55	0	45 <sup>b</sup>	151	45 <sup>b</sup>	1.5 (0.1)	6.8 (1.6)	-0.5 (0.4)
tC ( <b>7</b> )	48	6	45 <sup>b</sup>	148	45 <sup>b</sup>	2.4 (0.1)	7.3 (0.1)	0.2 (0.1)
tU ( <b>8</b> )	57	13	44 <sup>b</sup>	156	44 <sup>b</sup>	2.2 (0.1)	9.6 (1.5)	-0.7 (0.4)

<sup>a</sup> The puckering parameters  $P_N$ ,  $P_S$ ,  $\Psi_m^N$  and  $\Psi_m^S$  are given in degrees,  $\Delta H^\circ$  and  $\Delta G^\circ$  are in kJ mol<sup>-1</sup> and  $\Delta S^\circ$  are in J mol<sup>-1</sup> K<sup>-1</sup>. The standard deviations ( $\sigma$ ) of  $\Delta H^\circ$ ,  $\Delta S^\circ$  and  $\Delta G^\circ$  are given in parentheses.

<sup>b</sup> The pseudorotational parameter was kept fixed during iterative optimisation procedure.

and back-calculated  ${}^3J_{\text{HH}}$  (root-mean-square error < 0.06 Hz,  $\Delta J^{\text{max}} < 0.2$  Hz). Geometries of N-type conformers in **5–8** were characterised by the puckering between C3'-*endo*, C2'-*exo* and C3'-*endo* canonical forms ( $0^\circ < P_N < 13^\circ$ ), whereas their partners in the S-region of conformational space exhibited puckering intermediate between C2'-*endo*, C1'-*exo* and C2'-*endo* canonical forms ( $148^\circ < P_S < 158^\circ$ ) (Table IV). The maximum puckering amplitude ( $\Psi_m$ ) was between 44 and 45°.

*Ab initio Evaluation of the Puckering of 4'-Thiopentofuranose Moieties Supports the Drive of N  $\rightleftharpoons$  S Equilibrium in 1–8 towards N by S-C-N Anomeric Effect*

The shortening of the S4'-C1' bond between 0.1 and 1.1 pm, the lengthening of the C1'-N bond between 1.4 and 2.2 pm and opening of the S4'-C1'-N bond angle between 0.3 and 1.8° in HF/6-31G\*\* optimised geometries of tdG (**2**), tdU, tG (**6**) and tU (**8**) in N- compared to S-type pseudorotamers suggests more efficient delocalisation of the lone pair electrons on S4' to antibonding  $\sigma_{\text{C1'-N}}^*$  orbital in the N-type pseudorotamers (Table V). Our *ab initio* calculations unequivocally substantiate the existence of S-C-N anomeric effect in 4'-thionucleosides.

The phase angles of pseudorotation ( $P$ ) obtained from *ab initio* molecular orbital calculations at HF level of theory are very similar to the values

TABLE V  
Selection of bond lengths and bond angles from HF/6-31G\*\* optimised geometries<sup>a</sup>

Compd.	Conformational region <sup>b</sup>	Bond lengths			Bond angles	
		(C4'-S4')	(S4'-C1')	(C1'-N)	(S4'-C1'-N)	(C4'-S4'-C1')
tdG (2)	North	183.4	182.8	145.9	112.9	94.6
	East	181.8	183.0	144.2	112.5	89.2
	South	183.3	183.7	144.5	112.0	94.1
tdU	North	183.4	182.6	147.9	114.0	94.7
	East	181.9	183.2	145.5	112.3	89.0
	South	183.3	183.7	146.0	112.2	94.1
tG (6)	North	183.1	182.8	145.6	112.8	94.6
	East	181.8	182.5	143.9	112.3	89.5
	South	183.8	182.9	144.1	112.5	93.9
tU (8)	North	183.2	182.6	147.6	114.1	94.6
	East	182.0	182.4	145.1	112.8	89.3
	South	184.0	183.0	145.4	113.3	93.6

<sup>a</sup> Bond lengths are in pm, bond angles are in degrees.

<sup>b</sup> Other conformational degrees of freedom were in the starting geometries as follows:  $\gamma$ [O5'-C5'-C4'-C3'] = 180°,  $\zeta$ [H-O5'-C5'-C4'] = 180°,  $\varepsilon$ [C4'-C3'-O3'-H] = -60°,  $\varepsilon$ [C3'-C2'-O2'-H] = -60° for North and  $\varepsilon'$  = 60° for South pseudorotamers, and  $\chi$ [O4'-C1'-N9-C4/C2] = 180°. All the rotamers were completely freely optimised and were in the optimised structures found in the  $\gamma^{trans}$ ,  $\zeta^{trans}$ ,  $\varepsilon^{minus}$  and *anti* regions within  $\pm 10^\circ$  of the starting torsion angles.

that are characteristic for natural 4'-oxonucleosides. The extent of puckering expressed by maximum puckering amplitude ( $\Psi_m$ ) is however increased in 4'-thionucleosides up to 51°. For comparison, the average  $\Psi_m$  from X-ray crystal structures in their 4'-oxo analogues is 39°.

Our completely free optimisations of MeS-CH<sub>2</sub>CH<sub>2</sub>-OH at MP2/6-311++G\*\* level have shown the stabilisation of *trans* (179.9°) over *gauche* (-63.5°) conformer by 1.4 kJ mol<sup>-1</sup>.

## DISCUSSION

The conformational analysis of <sup>3</sup>J<sub>HH</sub> coupling constants in **1-8** has shown a slight bias of up to 70% towards South conformers (148° < P<sub>S</sub> < 185°, *i.e.* intermediate between C2'-*endo*, C1'-*exo* and C2'-*endo*, C3'-*exo* canonical forms) which are in conformational equilibrium with North forms (0° < P<sub>N</sub> < 20°, *i.e.*

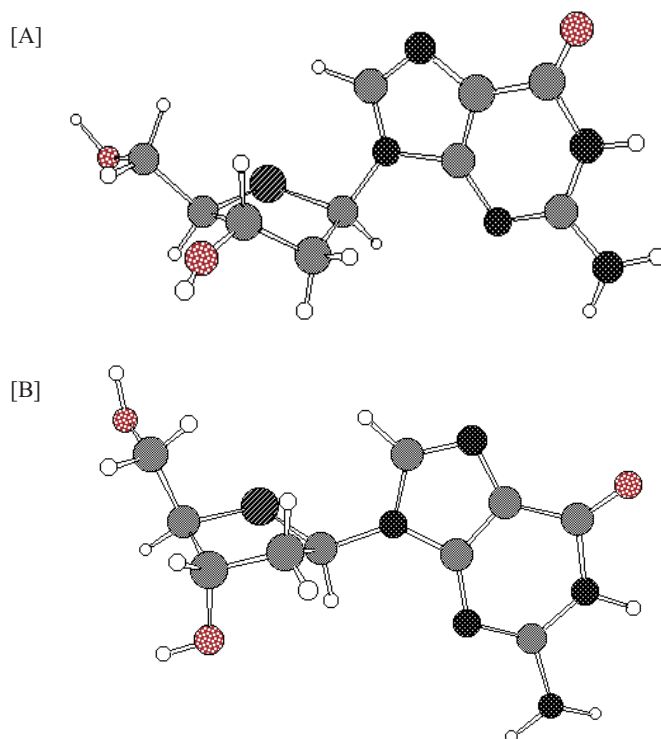


Figure 1. North ( $\approx$ C3'-*endo*, C2'-*exo*) and South ( $\approx$ C3'-*exo*, C2'-*endo*) conformers of tdG (**2**) showing the relative orientations of the exocyclic substituents on 4'-thiopentofuranosyl moiety. Both structures are the result of completely free optimisations at HF/6-31G\*\* level in the North ( $P_N = 2.1^\circ$ ,  $\psi_m^N = 45.9^\circ$ ) in panel [A] and in the South ( $P_S = 172.6^\circ$ ,  $\psi_m^S = 46.4^\circ$ ) in panel [B] regions of the conformational space.

intermediate between C3'-*endo*, C2'-*exo* and C3'-*endo* canonical forms). Thermodynamics of  $N \rightleftharpoons S$  pseudorotational equilibria in **1–8** can be explained by the competing steric and electronic effects of the following exocyclic substituents: nucleobase, 4'-CH<sub>2</sub>OH, 2'- and 3'-hydroxy groups.

(1) Purine and pyrimidine nucleobases drive  $N \rightleftharpoons S$  equilibrium in **1–8** towards N by S4'-C1'-N9/1 anomeric effect, where the nucleobase occupies pseudoaxial orientation (Figure 1A). It is however opposed by steric interactions, which are determined by the shape and size of aglycon. Steric hindrance of the nucleobase is expected to be minimised in the S-type pseudorotamers, where it occupies pseudoequatorial orientation (Figure 1B).

(2) 4'-CH<sub>2</sub>OH group drives  $N \rightleftharpoons S$  equilibrium in **1–8** towards N where it occupies pseudoequatorial orientation.

(3) 3'-hydroxy group drives  $N \rightleftharpoons S$  equilibrium in **1–8** towards N where it occupies pseudoequatorial orientation (Figure 1A). The energetic preferences of [S4'-C4'-C3'-O3'] fragments that were estimated from linear calibration graphs<sup>11</sup> correlating the energetics of *gauche* effects of [O4'-C4'-C3'-X3'] fragments in 3'-substituted-2',3'-dideoxythymidines with a group electronegativity of the 3'-substituent<sup>11</sup> has enabled us to predict that [S-C-C-O] fragment prefers *trans* conformation over *gauche* between 0.9 and 1.0 kJ mol<sup>-1</sup>. It is noteworthy that these estimates are in excellent agreement with our *ab initio* relative conformational energies of MeS-CH<sub>2</sub>CH<sub>2</sub>-OH. We have used 1 kJ mol<sup>-1</sup> as our best estimate for the preference of [S4'-C4'-C3'-O3'] fragments for *trans* over *gauche* conformations in **1–8**. The increased populations of  $\gamma^-$  rotamers in **1–8** in comparison to natural nucleosides are in full accord with the absence of *gauche* effect of [S4'-C4'-C5'-O5'] fragment (Table III).

*S-C-N Anomeric Effect in 1–4 is Weaker than the Corresponding O-C-N Anomeric Effect in 2'-Deoxynucleoside Counterparts*

The pairwise comparisons of populations of S-type conformers in **1–4** and in their 4'-oxo counterparts show higher preference of 13 and 5 percentage points for N-type pseudorotamers in tdA (**1**) and tdG (**2**) compared to dA and dG at 298 K, respectively (Figure 2A). In contrast, pyrimidine nucleosides show slightly higher preference of 1 and 5 percentage points for S-type sugar conformation in tdC (**3**) and tdT (**4**) in comparison to dC and T, respectively (Figure 2A). In addition, we have compared thermodynamics of  $N \rightleftharpoons S$  pseudorotational equilibria in **1–4** and in their 4'-oxo analogues and observed the stabilisation of N-type conformation by  $\Delta\Delta H_{\text{tot}}^\circ$  of 5.0 and 1.8 kJ mol<sup>-1</sup> in tdA (**1**) and tdG (**2**) in comparison with dA and dG, respectively (Figure 2B). The pairwise comparisons of  $\Delta H^\circ$  in tdC (**3**) and tdT (**4**) with dC and T show stabilisation of S-type conformation by  $\Delta\Delta H_{\text{tot}}^\circ$  of -0.2 and -0.9 kJ mol<sup>-1</sup> in 4'-thionucleosides, respectively. The differences in  $\Delta\Delta H_{\text{tot}}^\circ$  for 2'-deoxy analogues originate from the changes in several stereoelectronic effects due to the replacement of O4' with S4' that could be expressed by (2):

$$\Delta\Delta H_{\text{tot}}^\circ = \Delta GE + \Delta AE + \Delta SE(\text{aglycon}) + \Delta SE(4'\text{-OH}) \quad (2)$$

$\Delta GE$  is the change in energetics of [S4'-C4'-C3'-O3'] fragment in **1–4** compared to [O4'-C4'-C3'-O3'] fragment in natural counterparts. [O4'-C4'-C3'-O3'] fragment stabilises S-type sugar conformation by -7.3 kJ mol<sup>-1</sup> in natural 2'-deoxynucleosides,<sup>15</sup> while [S4'-C4'-C3'-O3'] fragment in **1–4** stabilises N-type sugar conformation by 1 kJ mol<sup>-1</sup>. The replacement of O4' with S4' therefore results in differential stabilisation of N-type pseudorotamers by 8.3 kJ mol<sup>-1</sup> due to [S4'-C4'-C3'-O3'] fragment in **1–4** in comparison to natural

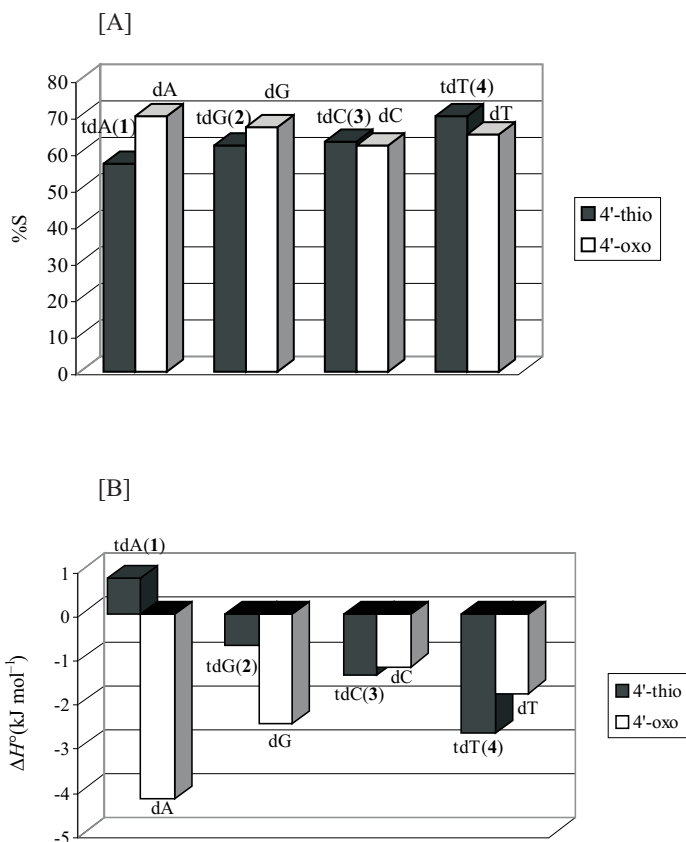


Figure 2. Pseudorotational  $N \rightleftharpoons S$  equilibrium in 2'-deoxy-4'-thionucleosides **1–4** and in their natural 4'-oxo counterparts<sup>15</sup> at 298 K. Comparison of population of South-type conformers as a function of nucleobase in panel [A] and  $\Delta H^\circ$  values in panel [B].

2'-deoxynucleosides. The subtraction of  $8.3 \text{ kJ mol}^{-1}$  from  $\Delta\Delta H_{\text{tot}}^\circ$  gives  $-3.3$ ,  $-6.5$ ,  $-8.5$  and  $-9.2 \text{ kJ mol}^{-1}$  stabilisation of S-type pseudorotamers for tdA (**1**)/dA, tdG (**2**)/dG, tdC (**3**)/dC and tdT (**4**)/T pairs, respectively. These  $\Delta\Delta H^\circ$  values can be attributed to: (i) the weakening of the anomeric effect in **1–4** in comparison to their 4'-oxo natural counterparts ( $\Delta AE$ ), (ii) the differences in the steric effect of heterocyclic aglycon ( $\Delta SE(\text{aglycon})$ ) and (iii) the steric effect of 4'-CH<sub>2</sub>OH group ( $\Delta SE(4\text{'-OH})$ ). The steric effect of heterocyclic aglycon, which stabilises S-type pseudorotamers is reduced in **1–4**, because S4'-C1' bonds are *ca.* 40 pm longer than O4'-C1' bonds. We should therefore observe a smaller stabilisation of S-type pseudorotamers in **1–4** compared to natural nucleosides if only the steric effect of aglycon was considered.

Similarly, C4'-S4' bonds are *ca.* 40 pm longer than C4'-O4' bonds and therefore N-type pseudorotamers are less stabilised in **1–4** compared to their 4'-oxo counterparts if only the steric effect of 4'-CH<sub>2</sub>OH groups is considered. The above steric effects are therefore opposing each other and the net effect in **1–4** in comparison to 4'-oxo analogues is probably small. We have however observed the preferential  $\Delta\Delta H^\circ$  stabilisation of S-type pseudorotamers in 2'-deoxy-4'-thionucleosides in comparison to their 4'-oxo analogues which leads to the conclusion that the  $n_{S4'} \rightarrow \sigma_{C1'-N}^*$  interactions in **1–4**, which drive  $N \rightleftharpoons S$  equilibria towards N are weaker than  $n_{O4'} \rightarrow \sigma_{C1'-N}^*$  interactions in natural 2'-deoxynucleosides. Although our current data set does not allow separation of individual contributions in Eq. (2) the  $\Delta\Delta H^\circ$  values of  $-3.3$ ,  $-6.5$ ,  $-8.5$  and  $-9.2$  kJ mol<sup>-1</sup> in **1–4**, respectively clearly indicate that S4'-C1'-N9 anomeric effect in **1–4** is weaker than O4'-C1'-N9 anomeric effect in their 4'-oxo counterparts. The above estimates of  $\Delta\Delta E$  in Eq. (2) also indicate that the drive of  $N \rightleftharpoons S$  equilibrium towards N upon replacement of O4' with S4' is weakened more with pyrimidine than with purine nucleobases.

*S-C-N Anomeric Effect is Stronger in Purine than in Pyrimidine  
4'-Thionucleosides*

The comparative analysis of  $\Delta H^\circ$  in **1–4** suggests that S4'-C1'-N9/1 anomeric effect increases in the following order: thymine < cytosine < guanine < adenine (Table IV and Figure 2B). The above order is reversed to what has been found for O4'-C1'-N9/1 anomeric effects in natural nucleosides (Figure 2B).<sup>4,5,15</sup> In natural 2'-deoxynucleosides the drive of their  $N \rightleftharpoons S$  equilibria towards N by the nucleobase increases in the following order: adenine < guanine < thymine < cytosine < uracil.<sup>4,5,15</sup>

*N  $\rightleftharpoons$  S Pseudorotational Equilibria in 4'-Thionucleosides **5–8** and in their  
4'-Oxo Counterparts*

$N \rightleftharpoons S$  pseudorotational equilibrium in 4'-thioribonucleosides **5–8** is characterised by a very similar population of both pseudorotamers at 298 K (Table IV and Figure 3A). There is considerable stabilisation of N-type pseudorotamers by  $\Delta H^\circ$  in **5–8**, which is opposed by entropy components of comparable strength (Table IV).

The  $N \rightleftharpoons S$  equilibria in tA (**5**) and tG (**6**) exhibit additional preference of 13 and 11 percentage points for N-type pseudorotamers at 298 K in comparison to A and G, respectively (Figure 3A). In contrast, pyrimidine ribonucleosides show higher population of S-type pseudorotamers by 11 and 10 percentage points in tC (**7**) and tU (**8**) in comparison with C and U, respectively. There is a large  $\Delta\Delta H^\circ$  of 7.5 and 4.7 kJ mol<sup>-1</sup> stabilising N-type conformation in tA (**5**) and tG (**6**) in comparison with A and G, respectively

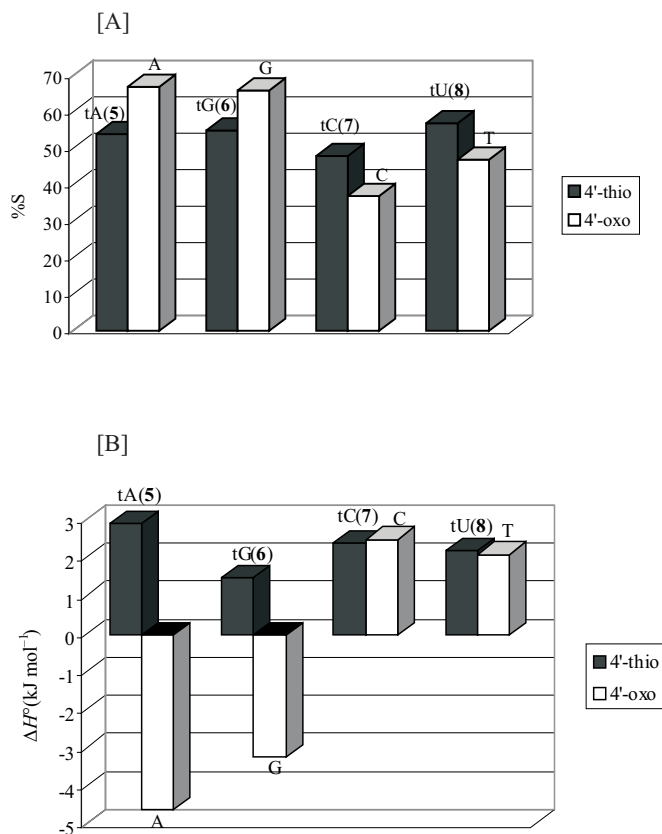


Figure 3. Pseudorotational  $N \rightleftharpoons S$  equilibrium in 4'-thioribonucleosides **5–8** and in natural ribonucleosides<sup>15</sup> at 298 K. Comparison of population of South-type conformers as a function of nucleobase in panel [A] and  $\Delta H^\circ$  values in panel [B].

(Figure 3B). The comparison of  $\Delta H^\circ$  values in tC (**7**) and tU (**8**) with their 4'-oxo counterparts C and U, respectively shows comparable stabilisation of N-type pseudorotamers with differences being within the error limits.  $\Delta H^\circ$  of  $N \rightleftharpoons S$  equilibria in **5–8** are all positive whereas their purine 4'-oxo analogues exhibit negative  $\Delta H^\circ$  values and the preference for S-type sugar conformation (Figure 3B). In contrast, 4'-oxo pyrimidine counterparts exhibit preference for N-type conformation which has been attributed to: (i) stronger O4'-C1'-N9/1 anomeric effect (stabilises N) of pyrimidine than purine nucleosides, and (ii) weaker *gauche* effect of [N9/1-C1'-C2'-O2'] fragments (stabilises S) in pyrimidine nucleosides.<sup>4</sup> [N9/1-C1'-C2'-O2'] fragments stabilise S-type pseudorotamers by  $\Delta H^\circ$  of  $-6.9$  and  $-2.9$  kJ mol<sup>-1</sup> in natural 4'-oxo purine and pyrimidine ribonucleosides, respectively.<sup>15</sup> The *gauche* effect of

[O3'-C3'-C2'-O2'] fragment does not preferentially stabilise N- over S-type conformers in **5–8**. [S4'-C1'-C2'-O2'] and [S4'-C4'-C3'-O3'] fragments prefer *trans* over *gauche* conformation, which are achieved in S- and N-type sugar conformations of **5–8**, respectively. As they oppose each other in the drive of N  $\rightleftharpoons$  S equilibrium we can assume that they do not preferentially stabilise N- over S-type conformers in **5–8**. Reasonable assumption that *gauche* effect of [N9/1-C1'-C2'-O2'] fragment is only slightly modulated in **5–8** in comparison to their 4'-oxo analogues leads to conclusion that S4'-C1'-N9/1 anomeric effect is weaker in pyrimidine than in purine 4'-thioribonucleosides. This observation is in complete agreement with data on **1–4** that S-C-N anomeric effect increases in the following order: thymine < cytosine < guanine < adenine.

## CONCLUSIONS

The conformational analysis of temperature-dependent  $^3J_{\text{HH}}$  coupling constants in a series of 4'-thionucleosides has enabled determination of the energetics of their North  $\rightleftharpoons$  South pseudorotational equilibria. The comparison of the conformational preferences and thermodynamic data on North  $\rightleftharpoons$  South equilibrium in 4'-thionucleosides and in their natural 4'-oxo counterparts has shown that S-C-N anomeric effect in the former is weaker than O-C-N anomeric effect in the latter. The  $\Delta\Delta H^\circ$  values between 2'-deoxy-4'-thio analogues and their 4'-oxo counterparts after accounting for the drive by 3'-OH group have been attributed to the weakening of the nucleobase-dependent S4'-C1'-N9/1 anomeric effect by 3.3, 6.5, 8.5 and 9.2 kJ mol<sup>-1</sup> in adenine, guanine, cytosine and thymine, respectively. Complementary high-level *ab initio* calculations substantiate the nucleobase-dependent S4'-C1'-N9/1 anomeric effect in the North pseudorotamers. In addition, S-C-N anomeric effect is stronger in purine than in pyrimidine 4'-thionucleosides and increases in the following order: thymine < cytosine < guanine < adenine, which is in contrast to natural nucleosides. Experimental  $\Delta H^\circ$  values indicate that the drive of North  $\rightleftharpoons$  South equilibrium towards North upon replacement of O4' with S4' is weakened more with pyrimidine than with purine nucleobases.

*Acknowledgement.* – We thank the Ministry of Science and Technology of the Republic of Slovenia (Grant No. Z1-8609-0104) for the financial support.

## REFERENCES AND NOTES

1. W. Saenger, *Principles of Nucleic Acid Structure*, Springer Verlag, New York, 1984.
2. C. Altona and M. Sundaralingam, *J. Am. Chem. Soc.* **94** (1972) 8205–8212.
3. C. Altona and M. Sundaralingam, *J. Am. Chem. Soc.* **95** (1973) 2333–2344.
4. J. Plavec, W. Tong, and J. Chattopadhyaya, *J. Am. Chem. Soc.* **115** (1993) 9734–9746.

5. C. Thibaudeau and J. Chattopadhyaya, *Stereoelectronic Effects in Nucleosides and Nucleotides and their Structural Implications*, Uppsala University Press, Uppsala, Sweden, 1999.
6. J. Plavec, N. Garg, and J. Chattopadhyaya, *J. Chem. Soc., Chem. Commun.* (1993) 1011–1014.
7. J. Plavec, L. H. Koole, and J. Chattopadhyaya, *J. Biochem. Biophys. Meth.* **25** (1992) 253–272.
8. L. H. Koole, J. Plavec, H. Liu, B. R. Vincent, M. R. Dyson, P. L. Coe, R. T. Walker, G. W. Hardy, G. S. Rahim, and J. Chattopadhyaya, *J. Am. Chem. Soc.* **114** (1992) 9936–9943.
9. J. Plavec, C. Thibaudeau, G. Viswanadham, C. Sund, and J. Chattopadhyaya, *J. Chem. Soc., Chem. Commun.* (1994) 781–783.
10. C. Thibaudeau, J. Plavec, K. A. Watanabe, and J. Chattopadhyaya, *J. Chem. Soc., Chem. Commun.* (1994) 537–540.
11. C. Thibaudeau, J. Plavec, N. Garg, A. Papchikhin, and J. Chattopadhyaya, *J. Am. Chem. Soc.* **116** (1994) 4038–4043.
12. J. Plavec, C. Thibaudeau, and J. Chattopadhyaya, *J. Am. Chem. Soc.* **116** (1994) 6558–6560.
13. C. Thibaudeau, J. Plavec, and J. Chattopadhyaya, *J. Am. Chem. Soc.* **116** (1994) 8033–8037.
14. J. Plavec, C. Thibaudeau, G. Viswanadham, A. Sandström, and J. Chattopadhyaya, *Tetrahedron* **51** (1995) 11775–11792.
15. J. Plavec, *Ph.D. Thesis*, Department of Bioorganic Chemistry, Uppsala University, Uppsala University Press, Uppsala, Sweden, 1995.
16. C. Thibaudeau, J. Plavec, and J. Chattopadhyaya, *J. Org. Chem.* **61** (1996) 266–286.
17. J. Plavec, C. Thibaudeau, and J. Chattopadhyaya, *Pure & Appl. Chem.* **68** (1996) 2137–2145.
18. I. Luyten, C. Thibaudeau, A. Sandström, and J. Chattopadhyaya, *Tetrahedron* **53** (1997) 6433–6464.
19. C. Thibaudeau, A. Foldesi, and J. Chattopadhyaya, *Tetrahedron* **54** (1998) 1867–1900.
20. I. Luyten, C. Thibaudeau, and J. Chattopadhyaya, *J. Org. Chem.* **62** (1997) 8800–8808.
21. C. Thibaudeau and J. Chattopadhyaya, *Nucleosides & Nucleotides* **17** (1998) 1589–1603.
22. I. Luyten, J. Matulic-Adamic, L. Beigelman, and J. Chattopadhyaya, *Nucleosides & Nucleotides* **17** (1998) 1605–1611.
23. C. Thibaudeau and J. Chattopadhyaya, *Nucleosides & Nucleotides* **16** (1997) 523–529.
24. C. Thibaudeau, A. Kumar, S. Bekiroglu, A. Matsuda, V. E. Marquez, and J. Chattopadhyaya, *J. Org. Chem.* **63** (1998) 5447–5462.
25. M. Polak, B. Mohar, J. Kobe, and J. Plavec, *J. Am. Chem. Soc.* **120** (1998) 2508–2513.
26. E. Juaristi and G. Cuevas, *Tetrahedron* **48** (1992) 5019–5087.
27. I. Tvaroska and T. Bleha (Eds.), *Anomeric and Exo-Anomeric Effects in Carbohydrate Chemistry*, Academic Press, San Diego, 1989, Vol. 47.
28. A. J. Kirby and N. H. Williams, in: G. R. J. Thatcher, (Ed.), *The Anomeric Effect and Associated Stereolectronic Effects*, 539 Ed., American Chemical Society, Washington, DC, 1993, pp. 55–69.

29. P. P. Graczyk and M. Mikolajczyk, *Top. Stereochem.* **21** (1994) 159–349.
30. M. Črnugelj, D. Dukhan, J. L. Barascut, J. L. Imbach, and J. Plavec, *J. Chem. Soc., Perkin Trans. 2* (2000) 255–262.
31. H. Yuasa and H. Hashimoto, *Rev. Heteroatom Chem.* **19** (1999) 35–65.
32. M. A. Clement and S. H. Berger, *Med. Chem. Res.* **2** (1992) 154–164.
33. L. Bellon, C. Leydier, J.-L. Barascut, G. Maury, and J.-L. Imbach, in: Y. S. Sanghvi and P. D. Cook, (Eds.), *Carbohydrate Modifications in Antisense Research*, 580 Ed., American Chemical Society, Washington, DC, 1994, pp. 68–79.
34. VNMR program, revision 6.1A, Varian Inc., Palo Alto, 1999.
35. C. Haasnoot, F. A. A. M. de Leeuw, D. Huckriede, J. van Wijk, and C. Altona, PSEUROT version 6.0, Leiden University, Leiden, Netherlands, 1993.
36. C. A. G. Haasnoot, F. A. A. M. de Leeuw, and C. Altona, *Tetrahedron* **36** (1980) 2783–2792.
37. C. Altona, R. Francke, R. de Haan, J. H. Ippel, G. J. Daalmans, A. J. A. Westra Hoekzema, and J. van Wijk, *Magn. Reson. Chem.* **32** (1994) 670–678.
38. The endocyclic torsion angles in **1–8** are defined as follows:  $\nu_0 \equiv [C4' - S4' - C1' - C2']$ ,  $\nu_1 \equiv [S4' - C1' - C2' - C3']$ ,  $\nu_2 \equiv [C1' - C2' - C3' - C4']$ ,  $\nu_3 \equiv [C2' - C3' - C4' - S4']$  and  $\nu_4 \equiv [C3' - C4' - S4' - C1']$ .
39. E. Diez, A. L. Esteban, F. J. Bermejo, C. Altona, and F. A. A. M. de Leeuw, *J. Mol. Struct.* **125** (1984) 49–65.
40. M. J. Frisch, G. W. Trucks, H. B. Schlegel, P. M. W. Gill, B. G. Johnson, M. A. Robb, J. R. Cheesman, T. Keith, G. A. Petersson, J. A. Montgomery, K. Raghavachari, M. A. Al-Laham, V. G. Zakrzewski, J. V. Ortiz, J. B. Foresman, J. Cioslowski, P. B. Stefanov, A. Nanayakkara, M. Challacombe, C. Y. Peng, P. Y. Ayala, W. Chen, M. W. Wong, J. L. Andres, E. S. Replogle, R. Gomperts, R. L. Martin, D. J. Fox, J. S. Binkley, D. J. Defrees, J. Baker, J. P. Stewart, M. Head-Gordon, C. Gonzalez, and J. A. Pople, *Gaussian 94*, Rev. D.1, Gaussian Inc., Pittsburgh, PA, 1995.
41. M. J. Frisch, G. W. Trucks, H. B. Schlegel, G. E. Scuseria, M. A. Robb, J. R. Cheesman, V. G. Zakrzewski, J. A. Montgomery, R. E. Stratman, J. C. Burant, S. Dapprich, J. M. Millam, A. D. Daniels, K. N. Kudin, M. C. Strain, O. Farkas, J. Tomasi, V. Barone, M. Cossi, R. Cammi, B. Mennucci, C. Pomelli, C. Adamo, S. Clifford, J. Ochterski, G. A. Petersson, P. Y. Ayala, K. M. Q. Cui, D. K. Malick, A. D. Rabuck, K. Raghavachari, J. B. Foresman, J. Cioslowski, J. V. Ortiz, B. B. Stefanov, G. Liu, A. Liashenko, P. Piskorz, I. Komaromi, R. Gomperts, R. L. Martin, D. J. Fox, T. Keith, M. A. Al-Laham, C. Y. Peng, A. Nanayakkara, C. Gonzalez, M. Challacombe, P. M. W. Gill, B. Johnson, W. Chen, M. W. Wong, J. L. Andres, M. Head-Gordon, E. S. Replogle, and J. A. Pople, *Gaussian 98*, Rev. A.5, Gaussian Inc., Pittsburgh, PA, 1998.
42. F. A. A. M. de Leeuw and C. Altona, *J. Comp. Chem.* **4** (1983) 428–437.
43. H. P. M. de Leeuw, C. A. G. Haasnoot, and C. Altona, *Isr. J. Chem.* **20** (1980) 108–126.

**SAŽETAK**

**Konformacijska NMR istraživanja pokazuju da je S-C-N anomerni efekt u tionukleozidima manji od O-C-N anomernog efekta u prirodnim nukleozidima**

*Martin Črnugelj i Janez Plavec*

Usporedbeno istraživanje pseudorotacijske ravnoteže Sjever  $\rightleftharpoons$  Jug u 4'-tionukleozidima i u njihovim prirodnim 4'-okso srođnicima, s pomoću spektroskopije NMR i *ab initio* proračuna, pokazala su da je S-C-N anomerni efekt u prvima slabiji nego O-C-N anomerni efekt u drugima. Razlika vrijednosti  $\Delta H^\circ$  između 2'-deoksi-4'-tioanaloga i njihovih 4'-okso srođnika, kada se uzme u obzir efekt 3'-OH grupe, pripisuje se slabljenju nukleobazno-ovisnog S4'-C1'-N9/1 anomernog efekta za 3,3; 6,5; 8,5 i 9,2 kJ mol<sup>-1</sup> u adeninu, guaninu, citozinu i timinu. Pored toga S-C-N anomerni efekt jači je u 4'-tionukleozidima purinskog tipa nego u onima pirimidinskog tipa, a opada slijedećim redom: adenin > guanin > citozin > timin, što je suprotno poretku za prirodne nukleozide.